UC Davis
UC Davis Previously Published Works

Title
Photoinduced degradation from trace 1,8-diiodooctane in organic photovoltaics

Permalink
https://escholarship.org/uc/item/3165f7rv

Journal
Journal of Materials Chemistry C, 6(2)

ISSN
2050-7534

Authors
Jacobs, IE
Wang, F
Bedolla Valdez, ZI
et al.

Publication Date
2018

DOI
10.1039/c7tc04358a

Peer reviewed

eScholarship.org Powered by the California Digital Library
University of California

Volume 6 | Number 2 | 14 January 2018 | Pages 181–402

Journal of Materials Chemistry C

Materials for optical, magnetic and electronic devices

rsc.li/materials-c

ISSN 2050-7526

PAPER

Adam J. Moulé *et al.*

Photoinduced degradation from trace 1,8-diiodooctane in organic photovoltaics

Journal of
Materials Chemistry C

ROYAL SOCIETY OF CHEMISTRY

PAPER

View Article Online
View Journal | View Issue

Cite this: J. Mater. Chem. C, 2018, 6, 219

Photoinduced degradation from trace 1,8-diiodooctane in organic photovoltaics†

Ian E. Jacobs,[a] Faustine Wang,[b] Zaira I. Bedolla Valdez,[b] Alejandra N. Ayala Oviedo,[b] David J. Bilsky[a] and Adam J. Moulé *[b]

Published on 03 November 2017. Downloaded on 06/01/2018 01:07:18.

Received 24th September 2017,
Accepted 3rd November 2017

DOI: 10.1039/c7tc04358a

rsc.li/materials-c

1,8-Diiodooctane (DIO) is a high boiling point solvent additive commonly used to control the active layer morphology of bulk-heterojunction organic photovoltaic (OPV) films. OPV devices fabricated using DIO often show improved efficiency, but recent studies have suggested that light exposure may cause residual DIO to react with OPV materials. We use NMR to quantify the amount of residual DIO in bulk heterojunction (BHJ) layers, finding that after a typical thermal evaporator high vacuum cycle DIO is still easily observed. This suggests that most completed devices contain trapped DIO. While OPV devices processed without DIO remain stable, devices processed with DIO rapidly degrade under illumination, even if they had undergone sequential heating and vacuum steps to remove the DIO impurity. These results suggest that impurities that can act as radical initiators, such as DIO, can be detrimental even at concentrations as low as 20 ppm by mass.

Introduction

Bulk-heterojunction (BHJ) organic photovoltaics (OPV) have been heavily researched due to their potential for inexpensive solution-based manufacture.[1] Controlling the nanoscale morphology of the donor and acceptor phases in BHJs is crucial to obtaining high device efficiency, and has been a major topic of research.[2,3] In the past decade, the use of mixed solvents has become a popular method to control of the active layer morphology and obtain higher efficiencies.[4,5] In particular, 1,8-diiodooctane (DIO) has seen wide use as a dilute solvent additive, particularly in mixtures of low-band gap polymers and fullerenes.[6–12] In general, the higher boiling point solvent (*e.g.* DIO) is enriched as the lower boiling point solvent evaporates.[4,13,14] This change in solvent ratio is used to either emulsify (prevent phase separation) or selectively solubilize (cause phase separation) the donor acceptor mixture.[15]

There is no question that the use of DIO improves the initial morphology of many high efficiency mixtures. However, it is known that a substantial fraction of high boiling point solvent additives such as DIO can remain in the OPV layer and induce fullerene mobility and crystallization.[13,15] Even more troublingly, residual DIO has been shown to react with OPV materials upon heating or light exposure.[13,16] These reactions bleach the material's π–π^* absorption and are therefore expected to degrade its electronic properties.[16]

In this context, a relevant question is whether trace DIO affects the performance of completed devices and—most critically—at what concentrations it becomes problematic. Lifetime studies of OPV devices[17,18] have covered degradation due to oxidation of the metal electrodes,[19–21] the presence of O_2[22–25] or H_2O,[21,26–28] the effect of different hole and electron conducting layers,[29–31] and the presence of trace metals[32] or organic impurities.[31,33,34] However, to our knowledge no device studies have explored the role of photochemical reactions of trace solvent impurities. It has previously been claimed that exposure to high vacuum removes DIO, and that as a result DIO photoreactivity is only of concern in devices processed without high-vacuum steps.[16] In this article, we will refute this claim, showing that a significant volume of DIO remains in films even several hours after spin coating, and that this DIO is not fully removed by high vacuum. We observe signatures of doping in P3HT:DIO films exposed to light, indicating the presence of free iodine and suggesting additional device degradation mechanisms. Finally, we perform a device lifetime study, revealing that DIO-processed devices subjected to sequential heating and high-vacuum exposure still show rapid degradation under illumination, while remaining stable in the dark. We conclude that the presence of even sub-ppt concentrations of radical initiators such as DIO are strongly detrimental to OPV devices upon illumination, and should be phased out of use.

Results and discussion

DIO photoreactivity

Residual DIO has been shown to react with conjugated polymers *via* a UV-initiated radical reaction.[16] However, since radicals can attack a wide variety of functional groups, the photoreactivity of DIO appears to be a general effect in both polymers and

[a] Department of Materials Science, University of California, Davis, California, USA
[b] Department of Chemical Engineering, University of California, Davis, California, USA. E-mail: amoule@ucdavis.edu

† Electronic supplementary information (ESI) available. See DOI: 10.1039/c7tc04358a

This journal is © The Royal Society of Chemistry 2018

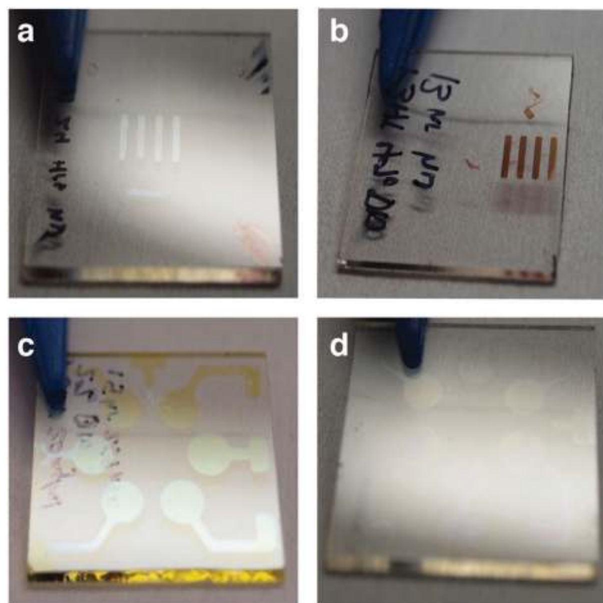

Fig. 1 Photos of films of (a) PCBM, (b) P3HT, (c) F8BT and (d) polystyrene cast from chlorobenzene (CB) and DIO (2% v/v) and cross-linked by exposure to a xenon arc lamp ($\sim$150 mW cm^{-2}, $t \approx$ 8 h, nitrogen atmosphere) through various shadow masks. Films were immersed in CB after exposure to remove unexposed (soluble) areas.

Published on 03 November 2017. Downloaded on 06/01/2018 01:07:18.

fullerenes. Fig. 1 shows photographs of polymer and small molecule films coated from 2% (v/v) DIO:chlorobenzene (CB) and exposured to a xenon arc lamp ($\sim$150 mW cm^{-2}, $t \approx$ 8 h) through a shadow mask. After exposure, the illuminated areas become insoluble and do not regain solubility upon heating; therefore the solubility reduction is due to cross-linking and not iodine doping.[35] Films exposed to light without DIO remain soluble. From the images in Fig. 1, it can be clearly seen that materials as diverse as [6,6]-phenyl C61 butyric acid methyl ester (a. PCBM), poly(3-hexylthiophene) (b. P3HT), poly(9,9-dioctylfluorene-*alt*-benzothiadiazole) (c. F8BT), and polystyrene (d. PS) are all easily cross-linked by spin coating from 2% v/v DIO:CB and subsequent exposure to white light. We therefore expect photoreactivity to be of concern in any organic electronic films processed with DIO.

Quantifying the DIO content of a coated film

In order to characterize the role of residual DIO on device lifetimes, we first must tackle the difficult task of quantifying the impurity concentration. *In situ* reflectometry and X-ray studies have been used to quantify solvent content *vs.* film thickness and observe crystal domain formation in BHJ mixtures, however these methods detect bulk thickness changes and are therefore relatively insensitive to trace impurities.[14,36–38] X-ray fluorescence (XRF) has also been used to measure residual DIO in OPV films.[16] It has been claimed that XRF can be used to detect DIO concentrations down to 1 ppm, however examination of noise in the XRF data suggests the true detection limit is orders of magnitude higher, as will be discussed below. In addition, XRF does not give a quantitative measurement of DIO concentration relative to polymer or fullerene, but instead only how the concentration of iodine changes for different processing conditions.

Nuclear magnetic resonance (NMR) spectroscopy is a simple method to determine the absolute concentration of residual DIO.[13] Chang *et al.* previously used NMR to quantify residual solvent additives in P3HT:PCBM layers before and after heat treatment.[13] We do not measure the layer in the solid state. Instead, after spin-coating and any processing steps (*e.g.* heating), the film is redissolved in $CDCl_3$ and the ratio of DIO *vs.* polymer or fullerene is quantified by comparing peak integration areas (which are proportional to molar concentration) using high-resolution solution-state NMR.

We use NMR to quantify the ratio of DIO to PCBM in samples spin-coated from 3% (v/v) DIO:CB after thermal or high vacuum treatments. Fig. 2a shows the molecular structures of P3HT, PCBM, and DIO, along with positions of the protons used to determine each species' molar ratio. These positions were chosen because their chemical shifts are well separated from other protons, however the results do not depend on which sites are used. ^{1}H NMR signals from these sites are shown in Fig. 2b for a film stored for 3 hours after spin-coating in a continuously purged N_2 glovebox at room temperature. Integration of these peaks indicate this film contained 1.9 DIO molecules for every PCBM molecule (27 wt% DIO). This is consistent with previous results,[13] and demonstrates that "dry" films processed from DIO still contain extremely high concentrations of DIO hours after spin coating.

It was previously reported that although significant quantities of DIO are present in spin coated films, exposure to high vacuum (required for thermal evaporation of metal back electrodes) removes this residual solvent.[16] This is not necessarily true. Fig. 2c shows the molar ratio of DIO to PCBM in films cast from 3% DIO:CB exposed to either a thermal evaporator high vacuum cycle (min. pressure 5×10^{-6} mbar, $t \approx$ 3 hours) or stored in a purged nitrogen glovebox for the same period. The CB:DIO evaporator film still shows a clear DIO signal (Fig. 2d) and a DIO concentration of 2 mol% relative to PCBM (0.4 wt% of the total film). This residue would be trapped in the film by the back electrode in completed devices.

To control for the possibility of film recontamination with DIO vapor in the glovebox after the evaporator cycle,[15] we also included a film processed from pure CB in the same evaporator cycle experiment. Fig. 2d shows the DIO ^{1}H NMR signal for these two samples. As expected, no DIO is visible in the BHJ film. Analysis of the signal to noise ratio (SNR) in our NMR data indicates a lower detection limit of 1 ppt DIO:PCBM. Since no DIO is detectable in the control sample, we conclude that the DIO observed in the CB:DIO evaporator sample is not due to contamination.

The high SNR of our NMR measurements compared to XRF explains why the previous XRF study did not detect DIO in films exposed to high vacuum.[16] The published XRF data shows a SNR of roughly 10 for films processed from 3% v/v DIO:CB. XRF is unable to determine absolute DIO concentration. However, if we assume a DIO concentration on the order of 1 : 1 DIO : PCBM (as observed by NMR for a 3% DIO film), we can infer a

 This journal is © The Royal Society of Chemistry 2018

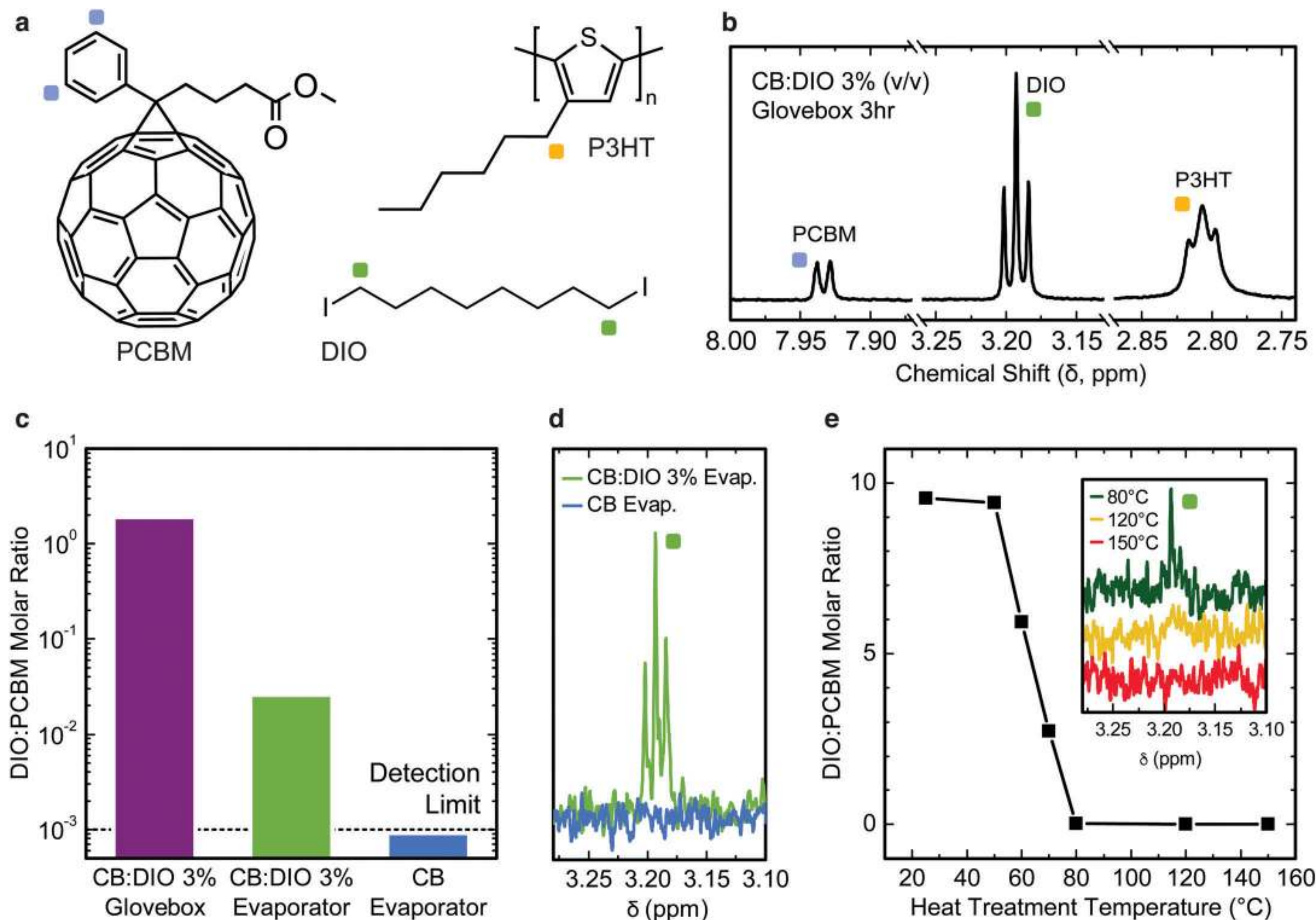

Fig. 2 Determination of residual DIO using ^{1}H NMR. (a) The molecular structure of P3HT, PCBM, and DIO, and markers showing which protons are used for the ^{1}H NMR molar concentration measurements. (b) ^{1}H NMR signals from sites marked in (a) from a P3HT/PCBM film cast from 3% (v/v) DIO:CB and stored in a purged N_2 glovebox for 3 hours. The y-axis is identical for all signals. (c) DIO : PCBM molar ratio for films exposed to the high vacuum cycle of a thermal evaporator for (t = 3 hours, min. pressure 5×10^{-6} mbar maintained for ~30 min) or stored in the glovebox for 3 hours. A film processed from pure CB was simultaneously tested to control for the possibility of DIO recontamination from the glovebox atmosphere. (d) Detail showing the DIO ^{1}H NMR signal from the films in (c) exposed to the evaporator vacuum cycle. (e) DIO : PCBM molar ratio in P3HT : PCBM films cast from 3% DIO:CB after heating for 5 min at various temperatures. Inset shows the DIO signal from the site marked in (a) for the three highest temperatures.

detection limit of around 10 mol% DIO (relative to PCBM) using XRF. This is not quite sensitive enough to detect the residual DIO in films exposed to high vacuum, and clearly nowhere near the 1 ppm sensitivity previously claimed.[16]

Heating the films before electrode deposition can remove most of the residual DIO. Fig. 2e shows the molar ratio between DIO and PCBM for films P3HT:PCBM cast from 3% DIO:CB after heating for 5 minutes on a hotplate at various temperatures. With no heat treatment, 5 minutes after spin coating the molar ratio of DIO to PCBM is 9.5 : 1, corresponding to a film which is 65% DIO by weight. 70 °C heat treatment still leaves the film with more DIO by mass than P3HT or PCBM individually, however, at 80 °C relatively little DIO remains (2 mol%) and at 120 °C the concentration is near the detection limit (0.016 mol%). No DIO is visible at 150 °C, although trace quantities (0.01 mass%) were previously observed after 150 °C heat treatment.[13] To prevent DIO recontamination,[15] we continuously purged the glovebox during these heating experiments. We conclude that heating is an effective method of removing most residual DIO from films, but that relatively high temperatures (>120 °C) are required and that sub-ppt concentrations may still be present.

The combined results depicted in Fig. 2 demonstrate that for typical device fabrication conditions, DIO is still present in films after evaporation of the back electrode. Together with the observed photoreactivity of DIO, there is a very real concern that DIO impurities could cause long term degradation of OPV devices.

Degradation mechanisms

The ability of DIO to cross-link conjugated polymers and fullerenes (shown in Fig. 1) is due to a radical reaction initiated by carbon–iodine bond cleavage.[16] This reaction reduces the absorptivity of conjugated polymers, presumably by disrupting

Published on 03 November 2017. Downloaded on 06/01/2018 01:07:18.

Published on 03 November 2017. Downloaded on 06/01/2018 01:07:18.

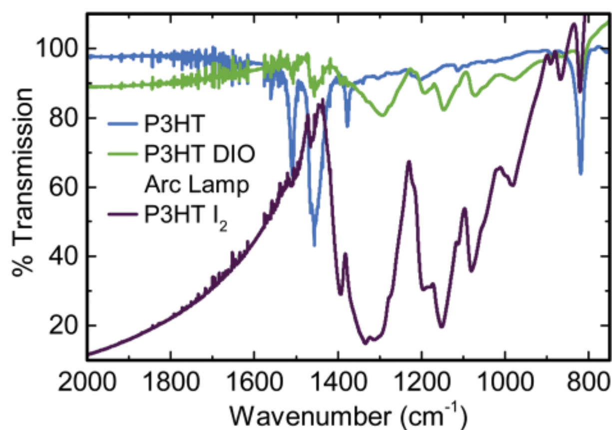

Fig. 3 FTIR spectra of P3HT films cast from CB (blue), 2% v/v DIO:CB exposed to a xenon arc lamp for 24 hours (green) and CB followed by exposure to I_2 vapor for approx. 1 minute (purple).

backbone conjugation,[16] and therefore is expected to degrade OPV device performance. However, the iodine released by this reaction may also interact with OPV devices by other mechanisms.

Fig. 3 shows FT-IR spectra of pristine P3HT, and P3HT cast from 2% DIO and exposed to a xenon arc lamp. The spectral region from 1350–900 cm^{-1} is devoid of peaks in the pure P3HT sample, but shows several new features in the cross-linked sample. For comparison, we also show a spectrum of P3HT that has been p-type doped by exposure to I_2 vapor. This I_2 doped sample shows the same new peaks as the DIO cross-linked sample, which have been previously assigned as IR-active vibrations (IRAV) resulting from charging of the polymer.[39,40] The broad absorption band above 1500 cm^{-1} in both the iodine doped and the DIO arc lamp sample is the P1 polaron band of P3HT.[40,41] These two features clearly indicate that iodine is produced by the photochemical reaction of DIO, and that this iodine in turn p-type dopes the P3HT film.

The presence of free iodine in OPV devices could be problematic for two reasons. Although the effect of doping on OPV devices at low concentrations is complex, films p-type doped at concentrations greater than 1 ppt generally perform poorly in OPV devices.[42,43] This is because doping-induced polarons are efficient exciton quenchers, and can increase non-radiative recombination. Iodine easily diffuses in and out of P3HT films, and therefore must exist in equilibrium between ionized states (*e.g.* I_3^- or I^-) and neutral I_2 within the film.[35,44] This presents a further issue, because I_2 is a fairly strong oxidizer and would be expected to react with the low workfunction electron-selective electrode. Depending on the product formed, this could alter the workfunction of the electrode, reducing the carrier selectivity of the interface,[45] form an interlayer which impedes electron transport,[46] or increase the device's series resistance. Therefore, several mechanisms exist by which the photoinduced reaction of DIO could reduce OPV performance.

Lifetime studies of OPV devices

In order to determine the effect of DIO reactivity on OPV devices, we fabricate a series of devices and monitor their current voltage (*J–V*) characteristics over several days under illumination (75 mW cm^{-2}, AM 1.5G spectrum). The device preparation

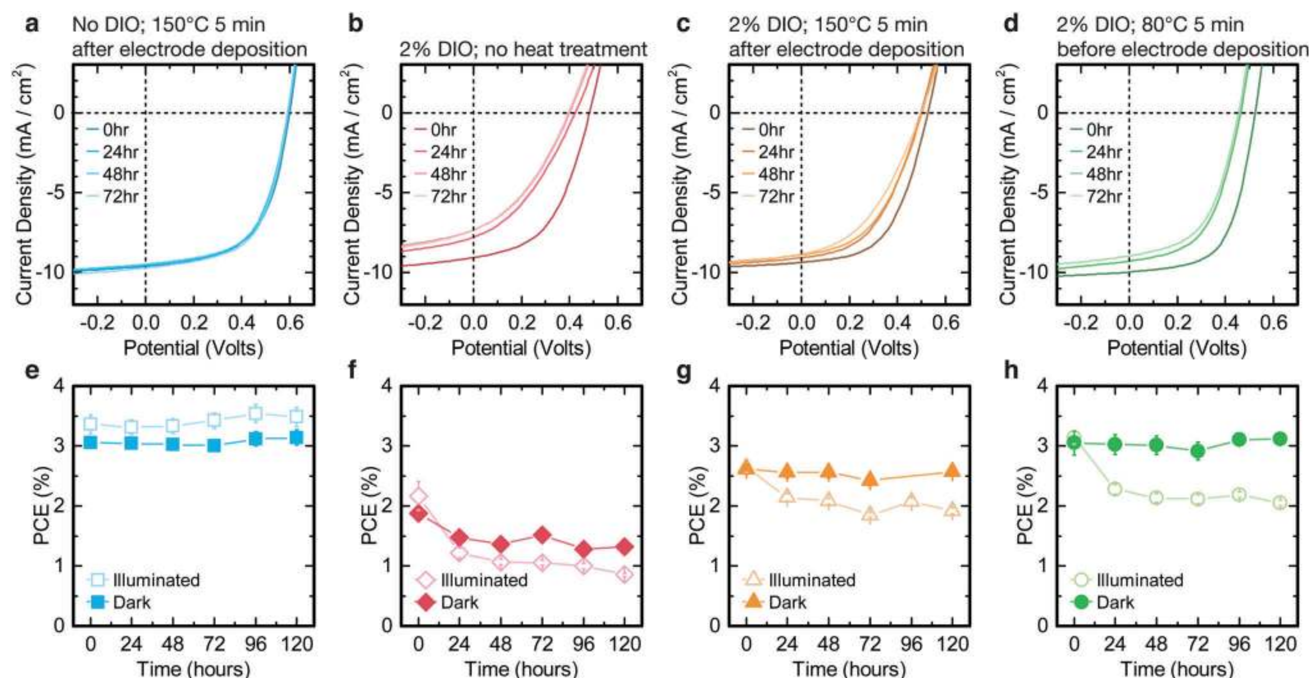

Fig. 4 (a–d) Current density/voltage measurements of P3HT/PCBM (1 : 1 mass ratio) OPV devices stored under 0.75 Sun AM 1.5G illumination for 0 to 72 h. Device preparation conditions for each sample are shown above; heat treatment was performed in a N_2 glovebox. Full data through 120 h for both illuminated and dark samples are shown in Fig. S1 (ESI†). (e–h) Long term PCE/time data for samples stored under illumination or in the dark for the devices above. Measurements are averaged over at least 5 working devices; error bars indicate standard deviation.

Published on 03 November 2017. Downloaded on 06/01/2018 01:07:18.

conditions are shown above each sample's *J–V* curves in Fig. 4a–d. A set of identical control samples was stored nearby in the same glovebox in the dark. During the experiment, the solar simulator bulb failed at around t = 90 h and was replaced within an hour, however the new bulb gave a higher light intensity (120 mW cm^{-2}). This slightly changed the shape of the *J–V* curves but did not significantly change the measured PCEs.[47–49] For clarity, only the *J–V* measurements before the bulb replacement are plotted; full data for both illuminated and dark samples are shown in the ESI.† Power conversion efficiencies for the illuminated and dark samples above are plotted as a function of time in Fig. 4e–h.

The sample without DIO depicted in Fig. 4a shows negligible change in the power conversion efficiency (PCE) over the 120 h of illumination (Fig. 4e). However, all other illuminated samples show a significant drop in PCE during the first 24 hours. In contrast, the samples stored in the dark fared much better, generally showing no significant signs of degradation over the course of our experiment. The initial drop in PCE, seen in only the illuminated samples containing DIO, must result from photochemical reaction of residual DIO. We note that this degradation behavior, consisting of rapid initial burn-in followed by relative stability, is consistent with previously observed radical reactions in OPV devices.[31,50]

The non-heat treated DIO sample (Fig. 4b), which should contain the most residual DIO (1 mol% DIO:PCBM; see Fig. 2) shows the most significant burn-in, losing nearly 50% of its PCE within the first day of illumination (Fig. 4f). This reduction is due to simultaneous reductions in short circuit density (J_{sc}), open circuit voltage (V_{oc}), and filling factor (FF). A more gradual reduction in PCE is also visible in the sample stored in the dark. However this is entirely due to a reduction in FF (Fig. S1f, ESI†) and therefore must result from a different mechanism; likely aggregation of PCBM facilitated by residual DIO.[13,15]

A more meaningful question is whether heat treatment can sufficiently reduce the DIO concentration and prevent degradation. Fig. 4c shows *J–V* characteristics from a device processed with DIO but otherwise identical to the device shown in Fig. 4a. Again, the illuminated sample shows a significant drop in PCE during the first 24 hours, while the dark devices remain stable; however, the reduction in PCE is much smaller than in the unheated DIO sample. As we showed in Fig. 2, heating to 150 °C is sufficient to reduce DIO concentration to below 1 ppt. However, the presence of the back electrode still appears to trap enough DIO in the film during heating to cause photodegradation.

We would expect heat treatment before electrode deposition to be a better strategy for removing residual solvent. Our NMR results in Fig. 2 indicate heat treatment at 80 °C for 5 minutes leaves a residual DIO concentration on the order of 1 mol% (relative to PCBM). Exposure to high vacuum results in a further 100-fold reduction in DIO concentration. Assuming the DIO evaporation rate scales similarly at lower total DIO concentrations, we expect completed devices annealed at 80 °C before electrode deposition to contain on the order of 100 ppm DIO:PCBM, or equivalently $\sim$20 ppm DIO by mass. Fig. 4d shows *J–V* characteristics for this device. Surprisingly, we still observe a clear reduction in both J_{sc} and V_{oc} during the first 24 hours of light exposure, resulting in a 28% reduction in PCE (Fig. 4h). The sample stored in the dark shows no degradation, with PCEs identical to the 'No DIO' dark samples (Fig. 4e). These results indicate that even extremely dilute DIO concentrations cause significant and rapid degradation to OPV devices.

We can rationalize the extreme sensitivity to dilute DIO impurities by considering that DIO acts as a radical initiator. Under dilute conditions, each photogenerated radical could potentially participate in many radical propagation reactions before finding another radical to terminate with. Therefore, extremely dilute concentrations of radical initiators can still cause significant harm to devices. To reach device lifespans of decades, any amount of residual DIO (or any other radical initiator) will be likely be problematic. Therefore, our results suggest that DIO and other solvents that could act as radical initiators should not be used in OPV devices, even when using thermal annealing or high vacuum steps.

Conclusions

In conclusion, we have examined the residual concentration of the solvent additive DIO in OPV films and studied the effects of photochemical reactions between DIO and the polymer and fullerene in OPV devices. We demonstrate that DIO will cross-link a variety of different organic samples when exposed to simulated solar irradiation. Quantitative measurements reveal high DIO concentrations in P3HT/PCBM films, and show that typical methods to remove DIO, like heat treatment or high vacuum exposure, do not generally remove all the DIO from films. We observe signatures of p-type doping in films after light exposure, indicating that the photogenerated iodine radicals subsequently dope the P3HT and should be capable of oxidizing low-workfunction electrodes. Finally we performed lifetime tests on OPV devices and show that samples containing even trace quantities of DIO degrade rapidly under illumination, while remaining stable in the dark. These results indicate that DIO is difficult to completely remove from polymer/fullerene films, and will cause OPV device photodegradation even at sub-ppt concentrations. We recommend the community move away from using DIO or other solvents capable of acting as radical initiators, even as low concentration solvent additives.

Experimental

Materials

P3HT (Plexcore XC-1350, MW = 52k) was obtained from Plextronics. PCBM was purchased from Nano-C. DIO (98+%, Cu stabilized) were purchased from Alfa Aesar. F8BT, PS, and solvents (chlorobenzene, chloroform) were purchased from Sigma-Aldrich. PEDOT:PSS (Clevios P VP AI 4083) was purchased from Heraeus. Deuterated chloroform was obtained from Cambridge Isotope Laboratories.

OPV device preparation

One square inch etched indium tin oxide (ITO)/glass substrates were sequentially cleaned in an ultrasonic bath with acetone, mucasal detergent (5%) and deionized water. Prior to use, the substrates were dried with nitrogen and UV-ozone treated for 20 min. P3HT/CB (20 mg mL^{-1}) and PCBM/CB (20 mg mL^{-1}) solutions were dissolved at 60 °C overnight. To prepare the OPV devices, PEDOT was filtered (0.2 μm) and spin-coated onto clean ITO substrates at 2500 rpm, followed by heating at 120 °C for 5 min to remove excess water. The substrates were immediately transferred to a glovebox (<1 ppm of H_2O, O_2) where they remained for all further fabrication and characterization. P3HT/PCBM films (1 : 1 mass ratio) were spin coated from 60 °C CB or 2% v/v DIO:CB solutions. Spinning speed was calibrated to yield 80 nm thick films as measured by profilometer (Veeco Dektak 150). Subsequently, 5 nm Ca followed by 150 nm Ag with an active area of 0.17 cm^2 were deposited by thermal evaporation at 5×10^{-6} Torr. Devices had heat treatment steps at different points during fabrication as described in the main text. Immediately after completion, all devices were encapsulated using degassed epoxy and a glass coverslip.

Devices were stored at open circuit in a glovebox either in the dark or under AM 1.5G illumination (Radiant Source Technology) at 75 mW cm^{-2} (t = 0–90 h) and 120 mW cm^{-2} (t = 90–120 h). Device J–V characteristics were measured every 24 hours using a sourcemeter (Keithley 2420) and the same solar simulator used for aging illumination. A reference silicon photovoltaic cell (VLSI Standards Inc.) was used to measure the light intensity before each set of measurements.

Spectroscopy

P3HT/PCBM films for NMR spectroscopy were spin coated from solutions containing 3% (v/v) DIO:CB onto glass substrates cleaned as described in the previous section. Films were approximately 80 nm thick. After processing (*i.e.* heat treatment or exposure to vacuum) the films were redissolved in $CDCl_3$. ^{1}H NMR spectra of these solutions were collected at 800 MHz on a Bruker Avance III spectrometer equipped with a cryoprobe. Acquisition times were <15 min (128 scans). Chemical shifts are referenced to TMS. Thick films of P3HT for FT-IR spectroscopy were drop cast onto glass substrates and measured in attenuated total reflectance (ATR) geometry (Bruker Tensor 27 with Pike MIRacle diamond/ZnSe ATR crystal).

Conflicts of interest

There are no conflicts to declare.

Acknowledgements

I. J. thanks the University of California Advanced Solar Technologies Institute/UC Solar (UC Office of the President MRPI #328386) for funding. Z. I. B. V. acknowledges the SENER-CONACyT program for postdoctoral fellowship funding.

References

1 C. J. Brabec, V. Dyakonov, J. Parisi and N. S. Sariciftci, *Organic photovoltaics: concepts and realization*, Springer Science & Business Media, 2013, vol. 60.
2 L. A. Perez, J. T. Rogers, M. A. Brady, Y. M. Sun, G. C. Welch, K. Schmidt, M. F. Toney, H. Jinnai, A. J. Heeger, M. L. Chabinyc, G. C. Bazan and E. J. Kramer, *Chem. Mater.*, 2014, **26**, 6531–6541.
3 A. J. Moulé and K. Meerholz, *Adv. Mater.*, 2008, **20**, 240–245.
4 F. L. Zhang, K. G. Jespersen, C. Bjorstrom, M. Svensson, M. R. Andersson, V. Sundstrom, K. Magnusson, E. Moons, A. Yartsev and O. Inganas, *Adv. Funct. Mater.*, 2006, **16**, 667–674.
5 A. J. Moulé and K. Meerholz, *Adv. Funct. Mater.*, 2009, **19**, 3028–3036.
6 J. Peet, J. Y. Kim, N. E. Coates, W. L. Ma, D. Moses, A. J. Heeger and G. C. Bazan, *Nat. Mater.*, 2007, **6**, 497–500.
7 J. K. Lee, W. L. Ma, C. J. Brabec, J. Yuen, J. S. Moon, J. Y. Kim, K. Lee, G. C. Bazan and A. J. Heeger, *J. Am. Chem. Soc.*, 2008, **130**, 3619–3623.
8 S. J. Lou, J. M. Szarko, T. Xu, L. Yu, T. J. Marks and L. X. Chen, *J. Am. Chem. Soc.*, 2011, **133**, 20661–20663.
9 M. S. Su, C. Y. Kuo, M. C. Yuan, U. S. Jeng, C. J. Su and K. H. Wei, *Adv. Mater.*, 2011, **23**, 3315–3319.
10 H. C. Liao, C. C. Ho, C. Y. Chang, M. H. Jao, S. B. Darling and W. F. Su, *Mater. Today*, 2013, **16**, 326–336.
11 K. Schmidt, C. J. Tassone, J. R. Niskala, A. T. Yiu, O. P. Lee, T. M. Weiss, C. Wang, J. M. J. Frechet, P. M. Beaujuge and M. F. Toney, *Adv. Mater.*, 2014, **26**, 300–305.
12 M. J. Zhang, X. Guo, W. Ma, S. Q. Zhang, L. J. Huo, H. Ade and J. H. Hou, *Adv. Mater.*, 2014, **26**, 2089–2095.
13 L. Chang, I. E. Jacobs, M. P. Augustine and A. J. Moulé, *Org. Electron.*, 2013, **14**, 2431–2443.
14 N. Shin, L. J. Richter, A. A. Herzing, R. J. Kline and D. M. DeLongchamp, *Adv. Energy Mater.*, 2013, **3**, 938–948.
15 L. Chang, H. W. A. Lademann, J.-B. Bonekamp, K. Meerholz and A. J. Moule, *Adv. Funct. Mater.*, 2011, **21**, 1779–1787.
16 B. J. Tremolet de Villers, K. A. O'Hara, D. P. Ostrowski, P. H. Biddle, S. E. Shaheen, M. L. Chabinyc, D. C. Olson and N. Kopidakis, *Chem. Mater.*, 2016, **28**, 876–884.
17 M. O. Reese, S. A. Gevorgyan, M. Jorgensen, E. Bundgaard, S. R. Kurtz, D. S. Ginley, D. C. Olson, M. T. Lloyd, P. Moryillo, E. A. Katz, A. Elschner, O. Haillant, T. R. Currier, V. Shrotriya, M. Hermenau, M. Riede, K. R. Kirov, G. Trimmel, T. Rath, O. Inganas, F. Zhang, M. Andersson, K. Tvingstedt, M. Lira-Cantu, D. Laird, C. McGuiness, S. Gowrisanker, M. Pannone, M. Xiao, J. Hauch, R. Steim, D. M. DeLongchamp, R. Roesch, H. Hoppe, N. Espinosa, A. Urbina, G. Yaman-Uzunoglu, J.-B. Bonekamp, A. J. J. M. van Breemen, C. Girotto, E. Voroshazi and F. C. Krebs, *Sol. Energy Mater. Sol. Cells*, 2011, **95**, 1253–1267.
18 F. C. Krebs, S. A. Gevorgyan and J. Alstrup, *J. Mater. Chem.*, 2009, **19**, 5442–5451.
19 N. Grossiord, J. M. Kroon, R. Andriessen and P. W. M. Blom, *Org. Electron.*, 2012, **13**, 432–456.

Published on 03 November 2017. Downloaded on 06/01/2018 01:07:18.

This journal is © The Royal Society of Chemistry 2018

View Article Online

Published on 03 November 2017. Downloaded on 06/01/2018 01:07:18.

20 B. Paci, A. Generosi, V. Rossi Albertini, P. Perfetti, R. de Bettignies and C. Sentein, *Chem. Phys. Lett.*, 2008, **461**, 77–81.

21 H. Klumbies, M. Karl, M. Hermenau, R. Rösch, M. Seeland, H. Hoppe, L. Müller-Meskamp and K. Leo, *Sol. Energy Mater. Sol. Cells*, 2014, **120**, 685–690.

22 M. S. Abdou, F. P. Orfino, Y. Son and S. Holdcroft, *J. Am. Chem. Soc.*, 1997, **119**, 4518–4524.

23 J. Schafferhans, A. Baumann, A. Wagenpfahl, C. Deibel and V. Dyakonov, *Org. Electron.*, 2010, **11**, 1693–1700.

24 A. Guerrero, P. P. Boix, L. F. Marchesi, T. Ripolles-Sanchis, E. C. Pereira and G. Garcia-Belmonte, *Sol. Energy Mater. Sol. Cells*, 2012, **100**, 185–191.

25 A. Seemann, T. Sauermann, C. Lungenschmied, O. Armbruster, S. Bauer, H.-J. Egelhaaf and J. Hauch, *Sol. Energy*, 2011, **85**, 1238–1249.

26 J. A. Hauch, P. Schilinsky, S. A. Choulis, S. Rajoelson and C. J. Brabec, *Appl. Phys. Lett.*, 2008, **93**, 103306.

27 V. M. Drakonakis, A. Savva, M. Kokonou and S. A. Choulis, *Sol. Energy Mater. Sol. Cells*, 2014, **130**, 544–550.

28 M. V. Madsen, S. A. Gevorgyan, R. Pacios, J. Ajuria, I. Etxebarria, J. Kettle, N. D. Bristow, M. Neophytou, S. A. Choulis, L. S. Roman, T. Yohannes, A. Cester, P. Cheng, X. W. Zhan, J. Wu, Z. Y. Xie, W. C. Tu, J. H. He, C. J. Fell, K. Anderson, M. Hermenau, D. Bartesaghi, L. J. A. Koster, F. Machui, I. Gonzalez-Valls, M. Lira-Cantu, P. P. Khlyabich, B. C. Thompson, R. Gupta, K. Shanmugam, G. U. Kulkarni, Y. Galagan, A. Urbina, J. Abad, R. Roesch, H. Hoppe, P. Morvillo, E. Bobeico, E. Panaitescu, L. Menon, Q. Luo, Z. W. Wu, C. Q. Ma, A. Hambarian, V. Melikyan, M. Hambsch, P. L. Burn, P. Meredith, T. Rath, S. Dunst, G. Trimmel, G. Bardizza, H. Mullejans, A. E. Goryachev, R. K. Misra, E. A. Katz, K. Takagi, S. Magaino, H. Saito, D. Aoki, P. M. Sommeling, J. M. Kroon, T. Vangerven, J. Manca, J. Kesters, W. Maes, O. D. Bobkova, V. A. Trukhanov, D. Y. Paraschuk, F. A. Castro, J. Blakesley, S. M. Tuladhar, J. A. Rohr, J. Nelson, J. B. Xia, E. A. Parlak, T. A. Tumay, H. J. Egelhaaf, D. M. Tanenbaum, G. M. Ferguson, R. Carpenter, H. Z. Chen, B. Zimmermann, L. Hirsch, G. Wantz, Z. Q. Sun, P. Singh, C. Bapat, T. Offermans and F. C. Krebs, *Sol. Energy Mater. Sol. Cells*, 2014, **130**, 281–290.

29 E. Voroshazi, B. Verreet, T. Aernouts and P. Heremans, *Sol. Energy Mater. Sol. Cells*, 2011, **95**, 1303–1307.

30 S. Nicht, H. Kleemann, A. Fischer, K. Leo and B. Lussem, *Org. Electron.*, 2014, **15**, 654–660.

31 W. R. Mateker and M. D. McGehee, *Adv. Mater.*, 2017, **29**, 1603940.

32 M. P. Nikiforov, B. Lai, W. Chen, S. Chen, R. D. Schaller, J. Strzalka, J. Maser and S. B. Darling, *Energy Environ. Sci.*, 2013, **6**, 1513–1520.

33 W. R. Mateker, J. D. Douglas, C. Cabanetos, I. T. Sachs-Quintana, J. A. Bartelt, E. T. Hoke, A. El Labban, P. M. Beaujuge, J. M. J. Frechet and M. D. McGehee, *Energy Environ. Sci.*, 2013, **6**, 2529–2537.

34 J. S. Moon, C. J. Takacs, Y. M. Sun and A. J. Heeger, *Nano Lett.*, 2011, **11**, 1036–1039.

35 I. E. Jacobs, J. Li, S. L. Berg, D. J. Bilsky, B. T. Rotondo, M. P. Augustine, P. Stroeve and A. J. Moulé, *ACS Nano*, 2015, **9**, 1905–1912.

36 J. J. van Franeker, M. Turbiez, W. Li, M. M. Wienk and R. J. Janssen, *Nat. Commun.*, 2015, **6**, 6229.

37 K. W. Chou, B. Yan, R. Li, E. Q. Li, K. Zhao, D. H. Anjum, S. Alvarez, R. Gassaway, A. Biocca, S. T. Thoroddsen, A. Hexemer and A. Amassian, *Adv. Energy Mater.*, 2013, **25**, 1923–1929.

38 A. J. Pearson, T. Wang, A. D. F. Dunbar, H. Yi, D. C. Watters, D. M. Coles, P. A. Staniec, A. Iraqi, R. A. L. Jones and D. G. Lidzey, *Adv. Funct. Mater.*, 2014, **24**, 659–667.

39 Y. H. Kim, D. Spiegel, S. Hotta and A. J. Heeger, *Phys. Rev. B: Condens. Matter Mater. Phys.*, 1988, **38**, 5490–5495.

40 R. Österbacka, C. P. An, X. M. Jiang and Z. V. Vardeny, *Science*, 2000, **287**, 839.

41 H. Sirringhaus, P. Brown, R. Friend, M. M. Nielsen, K. Bechgaard, B. Langeveld-Voss, A. Spiering, R. A. Janssen, E. Meijer and P. Herwig, *Nature*, 1999, **401**, 685–688.

42 I. E. Jacobs and A. J. Moulé, *Adv. Mater.*, 2017, **29**, 1703063.

43 Z. Shang, T. Heumueller, R. Prasanna, G. F. Burkhard, B. D. Naab, Z. Bao, M. D. McGehee and A. Salleo, *Adv. Energy Mater.*, 2016, **6**, 1601149.

44 I. E. Jacobs, J. Li, E. W. Aasen, J. Lopez, T. Fonseca, G. Zhang, P. Stroeve, M. P. Augustine, M. Mascal and A. J. Moulé, *J. Mater. Chem. C*, 2016, **4**, 3454–3466.

45 V. Mihailetchi, P. Blom, J. Hummelen and M. Rispens, *J. Appl. Phys.*, 2003, **94**, 6849–6854.

46 A. J. Moulé, M.-C. Jung, C. W. Rochester, W. Tress, D. LaGrange, I. E. Jacobs, J. Li, S. A. Mauger, M. D. Rail and O. Lin, *J. Mater. Chem. C*, 2015, **3**, 2664–2676.

47 P. Schilinsky, C. Waldauf, J. Hauch and C. J. Brabec, *J. Appl. Phys.*, 2004, **95**, 2816–2819.

48 L. J. A. Koster, V. D. Mihailetchi, R. Ramaker and P. W. M. Blom, *Appl. Phys. Lett.*, 2005, **86**, 123509.

49 L. J. A. Koster, V. D. Mihailetchi, H. Xie and P. W. M. Blom, *Appl. Phys. Lett.*, 2005, **87**, 203502.

50 A. Tournebize, A. Rivaton, J.-L. Gardette, C. Lombard, B. Pépin-Donat, S. Beaupré and M. Leclerc, *Adv. Energy Mater.*, 2014, **4**, 1301530.

This journal is © The Royal Society of Chemistry 2018